Atomic force microscopy combined with optical tweezers (AFM/OT)

F Pierini, K Zembrzycki, P Nakielski, S Pawłowska and T A Kowalewski

Department of Mechanics and Physics of Fluids, Institute of Fundamental Technological Research,
Polish Academy of Sciences, 02-106 Warsaw, ul. Pawinskiego 5B, Poland

E-mail: fpierini@ippt.pan.pl

CrossMark

Abstract

The role of mechanical properties is essential to understand molecular, biological materials, and nanostructures dynamics and interaction processes. Atomic force microscopy (AFM) is the most commonly used method of direct force evaluation, but due to its technical limitations this single probe technique is unable to detect forces with femtonewton resolution. In this paper we present the development of a combined atomic force microscopy and optical tweezers (AFM/OT) instrument. The focused laser beam, on which optical tweezers are based, provides us with the ability to manipulate small dielectric objects and to use it as a high spatial and temporal resolution displacement and force sensor in the same AFM scanning zone. We demonstrate the possibility to develop a combined instrument with high potential in nanomechanics, molecules manipulation and biological studies. AFM/OT equipment is described and characterized by studying the ability to trap dielectric objects and quantifying the detectable and applicable forces. Finally, optical tweezers calibration methods and instrument applications are given.

Keywords: atomic force microscopy/optical tweezers, optical trap stiffness calibration, force measurements, trap force, nanomanipulation

(Some figures may appear in colour only in the online journal)

1. Introduction

Force has a crucial role in physical, chemical and biological processes. The study of forces involved in molecular and nanomaterial interactions represents one of the most interesting contemporary challenges. Several techniques have been recently used to measure directly the forces required to unbind molecules, the surface forces responsible for nanoparticle stability, and to quantify mechanical properties of biological tissues and cells. Over the last few decades atomic force microscopy (AFM) has been the technique most frequently used to measure interaction forces of molecules and nanomaterials [1]. However, atomic force microscopy has limited use for examining small forces because its sensitivity is strictly dependent on the laser beam properties and the mechanical property of the probe [2]. Few techniques have successfully been developed to measure the force under the lower limit of detection of AFM in the last few years. Among them, optical tweezers stand out for their high resolution and flexibility [3]. Optical tweezers technique is based on trapping small particles using forces generated by laser radiation pressure. The concept of pressure from the propagation of light is at the core of optical tweezers technology and was hypothesized several centuries ago. Arthur Ashkin is the developer of 'single-beam gradient force trap', the technique that we now call optical tweezers [4]. He was able to demonstrate that it is possible to apply forces in the piconewton scale on small dielectric microspheres by focused laser beams using a high numerical aperture microscope objective [5].

The ability to manipulate single molecules attached to trapped micro or nanoparticles and to measure forces with femtonewton accuracy opened the way to the study of several important new topics [6–8]. Biologists were able to take immediate advantage of optical tweezers using this apparatus as a tool to study several biological systems and single molecules [9, 10]. Optical tweezers have been used for single molecule studies of biopolymers, where a single molecule of DNA,

RNA or protein has been twisted, stretched [11] and unfolded to measure its mechanical properties [12]. Furthermore, the growing interest in biophysics and the need to study DNA properties in greater details have prompted researchers to develop advanced experiments in which OT has been coupled with scanning probe microscopy [13, 14]. Optical tweezers have been used in studying intracellular organelles movement [15], in cell sorting [16] and flow virometry [17].

Over the years the use of optical tweezers has been opening new perspectives in several branches of physics. Optical tweezers have been used to study the movement of micro and nanoparticles in colloidal systems at different timescales starting from Brownian to ballistic motion [18] and the rotation of non-symmetric objects [19]. Optical trap can also be used to calculate the impact of surface modification on surface forces and drag coefficients of nanoparticles [20], to study rheology and the forces involved in single particle collisions and aggregation [21–24].

The aim of the present work is to demonstrate the possibility of extending the capability of a commercial AFM system by combining it with optical tweezers. It permits to obtain a high-quality imaging instrument able to trap and modify nanometric materials and to measure force in the subpiconewton scale. In this perspective, we have designed, built and calibrated an integrated AFM-optical tweezers system. We proved the instrument performance that allows us to manipulate single polystyrene particles. We analysed the quadrant photodiode detector noise and its response to the displacement of a particle from the centre of the trap. The movement of the piezo stage was used to measure the optical tweezers behaviour and to calculate trapping force using the drag-force calibration method. The calibration procedure was confirmed by comparing the previously obtained results, from the external force calibration, with those achieved using the equipartition method. The knowledge of optical trap stiffness is fundamental in single molecules, biological and single colloidal object studies to provide a comprehensive quantitative value of the forces involved in molecules and nanomaterials interactions.

An experiment in which the AFM/OT system was used to create a multi-particles structure, allowed us to prove the proposed instrument capability of acting as a nanomanipulator and to scan the produced structure with the AFM probe at the same time, generating a high resolution image of the manipulated sample. Finally, the instrument capability to detect forces with femtonewton accuracy was proved by analysing the interaction forces acting between single polystyrene particles in different environmental conditions.

2. Experimental setup and materials

2.1. Optical tweezers setup

A hybrid AFM-optical tweezers apparatus capable of trapping a single micrometric object and to measure forces with femtonewton resolution was built. Our optical tweezers instrument is based on the inverted microscope (IX71, Olympus Optical Co. Ltd, Tokyo, Japan) of an AFM system (Ntegra

Spectra, NT-MDT, Limerick, Ireland). A Nd:YAG 2 W diode pumped laser (Cobolt Rumba CW 1064 nm DPSSL, Cobolt, Solna, Sweden) combined with a series of dichroic mirrors, filters, beam expanders is employed to create an optical trap that could confine single objects in colloidal systems. Several factors contributed to the choice of trapping laser wavelength. Usually, biological matter like living cells has relative transparency in the near infrared region. Studies on cells have shown that the interaction with a laser beam in the range of wavelengths of 800 nm to 1100 nm does not affect cell growth [25]. A Nd:YAG laser source, able to generate a 1064 nm wavelength Gaussian beam, was chosen because it provides the suitable power, wavelength and profile to trap colloidal particles and biological material avoiding heat-related damage.

Three lasers are employed in these studies. These are 532 nm (*laser source* 1), 1064 nm (*laser source* 2), and 633 nm (*laser source* 3) in wavelengths (figure 1). The infrared laser path uses several mirrors to direct the beam into the objective aperture. A series of elements including *half-wave plate* 1, polarizer and a photodiode are used as a power regulator in order to generate a suitable beam to trap the object. The laser beam passes through a beam expander to form its appropriate diameter. The oil-immersion objective used (UPlanFl, Olympus Optical Co. Ltd, Tokyo, Japan) has a $100 \times$ magnification and a numerical aperture of 1.30. The back aperture of the microscope objective is overfilled by the Gaussian laser beam in order to generate a stable trap. A piezo stage is placed over the objective. Here the sample can be located in a suitable position to trap a single particle in 3D space near the focal point. Between the beam expander and the back aperture of the objective lens are five mirrors which provide necessary beam adjustments. There are, in addition, two other laser sources. The green 532 nm wavelength laser (Laser Source 1, NL202, Ekspla, Vilnius, Lithuania) is used to excite fluorescent materials for imaging purposes. *Beam expander* 1 is used to optimize the laser beam diameter and a series of mirrors to direct the beam to the sample using the same pathway as the trapping beam after the *dichroic mirror* 4. The images obtained using white light as well as those generated from the interaction between the fluorescent samples and the 532 nm laser beam are captured by the CMOS camera (HiCAM 500; Lambert Instruments, Leutingewolde, The Netherlands). An additional *filter* 1 is placed between the sample and the CMOS camera in order to filter out the scattered laser light interference from the resulting image.

The 633 nm red laser (*Laser source 3*, 25 LHP 991, Melles Griot, Irvine, California, USA) is the core of our most sensitive detection system. A series of mirrors guide the red laser beam to the back aperture of the objective and to the trapped particle, partly sharing pathway of the 532 nm and 1064 nm lasers. The backscattered light travels along the same optical path as the incident beam. *Dichroic mirror* 1 and *mirror* 3 allow the transmission of all the components of the rays in the opposite direction of the incident beam but *dichroic mirror* 4 filters out the green light. The backscattered beam arrives to the *filter* 2 passing through *a mirror* 8, *dichroic mirror* 9, *quarter-wave plate* 2 and *polarizing beam splitter* 1, where the infrared
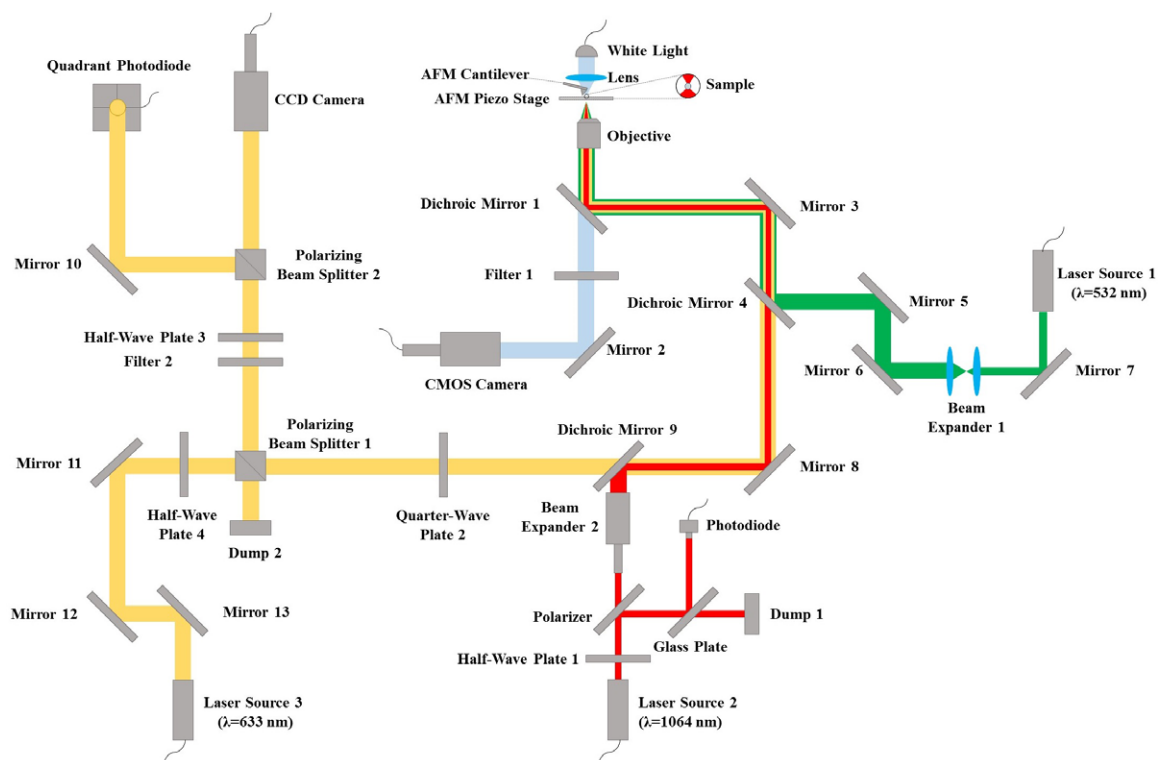
Figure 1. A sketch showing the scheme of the optical tweezers setup. A power regulator system composed of *half-wave plate* 1, *polarizer*, *glass plate*, *dump* 1 and a *photodiode*, and a *beam expander* 2 adjust the intensity and the shape of an infrared laser beam (red beam). The optical trap is created by a high-numerical aperture objective able to focus the laser beam over the piezo stage. The particle position detection uses a 633 nm laser (yellow beam) directed to the trapped particle. The backscattered light is collected to a *quadrant photodiode*. A third laser beam (green beam) is used to excite fluorescent materials for imaging purposes. The second detector is a *CMOS camera* used to obtain imaging of the trapped object.

radiation is filtered out. The CCD camera (CV-M10 RS, JAI, Yokohama, Japan) is used to get particle scattering images. The backscattered 633 nm laser light from the trapped particle is imaged onto a quadrant photodiode (QPD, S4349, Hamamatsu Photonics Inc., Hamamatsu, Japan) to evaluate position of the trapped object. For a particle perfectly centred in the trap, the resulting backscattered beam is directed to the middle of the quadrant photodiode. If the bead is displaced, the retracted beam points far from the centre of the detector. The quarter- and half-wave plates are used to generate a circularly polarized Gaussian beam and to control the detection laser power.

The base of our optical tweezers is an inverted microscope which is part of an atomic force microscope. This setup allows us to combine optical tweezers with AFM. The AFM piezo stage controlled by a computer gives the opportunity to displace the trapped particle and to control sample position with subnanometer accuracy. In order to decrease mechanical perturbations the instrument is mounted on an optical table with active vibration isolation. A computer is used to control the piezo stage movements, the light power and to collect and analyse numerical data.

The quantitative position and force analysis were carried out by measuring the shift of the backscattered light with a quadrant photodiode. The detector is made up of four different photodiodes arranged in a quadrant array. Every quadrant behaves like a single photodiode and generates an electrical current proportional to the intensity of light induced on it.

A specially built amplifier converts that current into voltage and amplifies it. The generated voltage, which is linearly proportional to the light, is measured by a data acquisition card (PCI-6036E, National Instruments Co., Austin, Texas, USA). The outputs from the quadrant photodiode are converted to voltage by a high speed, low-noise, high gain transimpedance amplifier. All single photodiode quadrants are treated separately and have their own dedicated signal path. The only exception is the reverse bias voltage applied to the common cathode. Reverse bias reduces the capacitance of the photodiodes and therefore increases frequency bandwidth and reduces noise. The bandwidth of this circuit is set to 50 kHz to match the bandwidth of the acquisition card.

The instrumental parameters control and data acquisitions are performed by LabVIEW (LabVIEW Professional Development System 2013 Version 13.0f2 32bit, National Instruments Co., Austin, Texas, USA), Nova (Nova, NT-MDT, Limerick, Ireland) and the supplied camera software. The collected data are exported to Matlab (Matlab 8.3 R2014a, The MathWorks Inc., Natick, Massachusetts, USA) and Origin (Origin 9.0, OriginLab Corp., Northampton, Massachusetts, USA) software for further processing and statistical treatments.

2.2. Materials

All chemicals were of analytical grade, purchased from commercial suppliers. The experiments were performed using

fluorescent polystyrene particles with diameter of 1.0 μm dispersed in aqueous solution (Fluoro-Max Dyed Red Aqueous Fluorescent Particles, Thermo Scientific Inc., Fremont, California, USA). The AFM topography was recorded using a conical tip shape cantilever (HA_NC, NT-MDT, Limerick, Ireland). The colloidal probe cantilever was built using a fluorescent polystyrene microsphere with diameters of 5.5 μm (Red Fluorescent Polymer Microspheres Duke Scientific Corporation, Palo Alto, California, USA), epoxy glue (Poxipol, Bripox, Warsaw, Poland) and a rectangular tipless cantilever (CSG 11/tipless, NT-MDT, Limerick, Ireland). The microfluidic channels were fabricated out of polydimethylsiloxane (PDMS, Sylgard 184, Dow Corning Corp., Midland, Michigan, USA) by soft lithography. Surface-oxidized cover glass, obtained by exposing cover slips (24 mm × 24 mm, Carl Roth GmbH, Karlsruhe, Germany) to oxygen plasma (Zepto B, Diener Electronics GmbH, Ebhausen, Germany), was used to seal the PDMS channels. Acrylamide (AAm, Sigma Aldrich, Poznan, Poland), N,N′-methylene bisacrylamide (BIS-AAm, 99.5%, Sigma Aldrich, Poznan, Poland), ammonium persulfate (APS, 98%, Sigma Aldrich, Poznan, Poland), N,N,N′,N′-tetramethylethylenediamine (TEMED, 99%, Sigma Aldrich, Poznan, Poland), 3-aminopropyltriethoxysilane (APTES, 98%, Sigma Aldrich, Poznan, Poland), potassium chloride (KCl, 99%, Sigma Aldrich, Poznan, Poland) and hexane (99%, Sigma Aldrich, Poznan, Poland) were used without further purification during the experiments. All solutions were prepared using ultra-pure water with conductivity of 0.056 μS cm^{-1}. Water was deionized using a Hydrolab HLP purification system (HLP 5UV, Hydrolab, Wiślina, Poland).

3. Experiments and discussions

3.1. Calibration

The calibration of optical tweezes is crucial in using this hybrid equipment as a quantitative sensor of forces. Even though the stiffness of optical tweezers is predictable by theoretical calculation, it nevertheless must be experimentally determined, because it is difficult to measure all the experimental parameters that should be included in the calculation. There are several methods to calibrate an optical tweezers apparatus.

In this section we show the methods used and discuss the results of the calibration of QPD looking at the output signals—particle displacement relationship and the force calibration of the instrument.

The optical tweezers stiffness was evaluated over the widest possible range of trapping laser power level, because we are aware of the importance of this technique to study also non-biological materials where the material damage due to the irradiation is negligible. Although the low cell damage induced by Nd:YAG 1064 nm laser [26] as well as the possibility to use high infrared laser power in biomolecules experiments [27] and the introduction of temperature controlled system have already been proven [28], a special attention was paid to explore the optical tweezers properties under 10 mW laser power level.
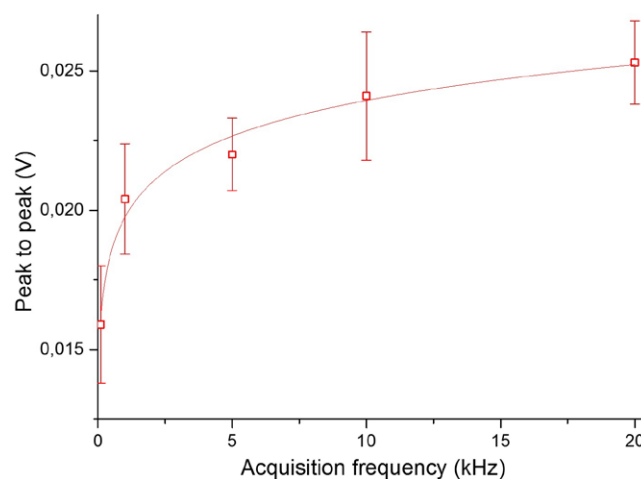

Figure 2. Instrumental noise highlighted as the peak to peak value of signal background for different acquisition frequencies and its best-fit. Data points represent an average of 40 experiments in which the signal was recorded for 2 s each single batch experiment. Error bars were estimated by using the standard deviation.

Before that, the detection system and optical trap calibration were performed, an electric optical power meter (Nova II with PD300-3W sensor, Ophir Optronics, Jerusalem, Israel) was placed perpendicularly in front of the microscope objective in order to determine the power of the beam that irradiate the sample at the trapped object plane. The power reaching the sample was calculated for all the lasers setups used in the described experiments.

3.1.1. Detection system calibration. The first step to calibrate the trap was the analysis of quadrant photodiode response. In order to adjust the sample rate we analysed the noise of the quadrant photodiode at several frequencies when a motionless particle was in the focal point. A dispersion of polystyrene spheres 1.0 μm in diameter in polyacrylamide gel was used to place a fixed polystyrene sphere in the centre of the trap and the 633 nm laser power was adjusted so that the total voltage of QPD was 4 Volts (V). The signals were recorded for 2 s at each single analysed sample rate. The recorded signals were analysed expressing the instrumental noise as peak-to-peak value. The lower the acquisition rate, the less noisy the output signal is (figure 2). At high acquisition frequencies the analyses were affected by the noise. At low frequency the QPD was not able to detect fast and small particle displacement, therefore the selected sample rate of the detection system was set up at a maximum of 10.0 kHz in order to reach the optimum signal-to-noise ratio and speed. The output signals of the quadrant photodiode are clearly exposed to several sources of noise. Electronic noise, mechanical, acoustic vibrations and laser instabilities can be minimized by applying some experimental precautions but it cannot be removed completely. However, a much higher peak-to-peak signal value is generated by the Brownian motion of trapped object.

In order to calibrate the optical tweezers using the backscattered light collecting sensor as particle position sensor we need to fully know the response of QPD as a function of bead displacement. A 1.0 μm diameter polystyrene particle stuck

in polyacrylamide gel was used to study the sensitivity of the quadrant photodiode. The bead was placed in the centre of the trap. The piezo stage, on which the sample was mounted, allowed us to move the polystyrene sphere with a stepwise motion. We recorded the values of S_x and S_y (quadrant photodiode signals related the particle displacements along the X axis and Y axis, respectively) and after each particle displacement generated by a small and quick piezo stage movement when the bead passed through the tweezers. The particle displacements were generated by a sequence of back and forth stage movements and the measurements were carried out starting from -100 nm to $+100$ nm. Each measurement point was repeated 100 times.

The presence of backscattered light pattern asymmetry is responsible for the small differences in sensitivity between X and Y direction as well as the non-linear response for bead displacements higher than 100 nm from the centre of the trap. The sensitivity of the quadrant photodiode is also affected by the ratio of light spot radius and QPD radius to the distance between the centre of the detector and the reflected beam.

3.1.2. External force calibration. The external force calibration method quantifies the amount of force applied by the trapping laser on the bead using a specific instrumental and environmental configuration. The analysis of the relationship between the particle position and the quantity of an applied external force on the trapped sphere under controlled condition is one of the most effective strategies to calibrate the trap. It is possible to calculate the trap stiffness by observing the particle displacement while applying on it a known external force. Hydrodynamic drag, resulting from an applied flow of water around the trapped particle, acted as the external force. The analysed colloidal system was confined in a PDMS channel sealed with a glass coverslip and the particle was trapped 5 μm far from the glass wall and at least 50 μm away from any surface. The experiment was performed at the system equilibrium in order to avoid any unexpected convective flow. The flow Reynolds number based on the particle diameter was below 10^{-3}. The results were corrected according to Faxen's law in order to take into consideration the effect of the wall proximity to the particles in the applied experimental conditions [20].

The flow of the fluid around the trapped sphere was applied by moving the piezo stage on which the channel was mounted. The external force was quantified using the method proposed by Mills *et al* [29], where the AFM piezo stage was moved at different constant velocities translating the chamber by steps of 100 μm in the X and Y direction. The system was analysed at several values of external force maintaining the step displacement constant and changing the stage velocity; at least 100 events were taken into account in the stiffness calculation in each analysed experimental condition. The optical tweezers stiffness was calculated at 15 different trapping laser power levels by analysing the recorded output signals of the QPD particle position detector. The results were averaged over few experiments repeated using the same experimental parameters. The trap stiffness increases linearly with the trapping

Table 1. Traversal escape force measured from 1.74 to 4.24 mW of trapping laser power.

Trapping laser power (mW)	Axes direction	Escape force (pN)	Escape force standard deviation (pN)
1.74	X	4.91	0.35
2.62	X	7.22	0.22
4.24	X	11.17	0.74
1.74	Y	4.89	0.11
2.62	Y	7.26	0.13
4.24	Y	10.89	0.18

laser intensity. The optical tweezers calibrations show the stiffness asymmetry caused by the polarization of the laser beam. These results are in agreement with theoretical and previous experimental results achieved by Rohrbach [30], where the relationship between the asymmetry coefficient and several experimental parameters (e.g. power and wavelength of laser and particle dimension) was proven.

When the piezo stage speed was increased above a certain threshold, the external force overcame the trapping laser force and the bead escaped from the optical tweezers. The escape force is defined as the highest force applicable to the trapped objects therefore it defines the upper force limits of optical tweezers. The higher the trapping laser power, the higher the escape force (table 1). We found that our optical tweezers system has a maximum escape force of 11.17 pN using a 4.24 mW trapping laser.

3.1.3. Equipartition calibration. The trapped bead oscillates randomly near the focal point of the laser beam when it is in thermal equilibrium. Therefore, the system can be considered a sphere in a harmonic potential. It is possible to estimate the trap stiffness by tracking the particle position and calculating the displacements from the average position point in a well-known thermal condition. The equipartition theorem defines the average translational kinetic energy of a particle for each translational degree of freedom as ½ $k_B T$ where k_B is the Boltzmann constant and T is the absolute temperature.

The displacements of a 1.0 μm polystyrene particle in water were recorded for 20 s with a fixed acquisition frequency (10.0 kHz) at several trapping laser power levels. The trap stiffness was calculated averaging 30 series of data acquisitions for each laser power settings (figure 3). The temperature of the fluid was evaluated using a pre-calibrated thermocouple sensor located few micrometres far from the analysed bead and assuming that the temperature in this point was similar to the trap temperature [31]. In this experiment the power of 1064 nm laser was set starting from 0.50 mW and then was gradually increased to 50.0 mW. We noticed that due to the temperature rising at high laser power level, the difference between the focal point where the particle is confined and the surrounding liquid created large convective instabilities in the system, forcing us to extend equilibration time. The temperature estimation has a crucial role in the equipartition calibration. The measured stiffness standard deviation rose in proportion to the laser power.
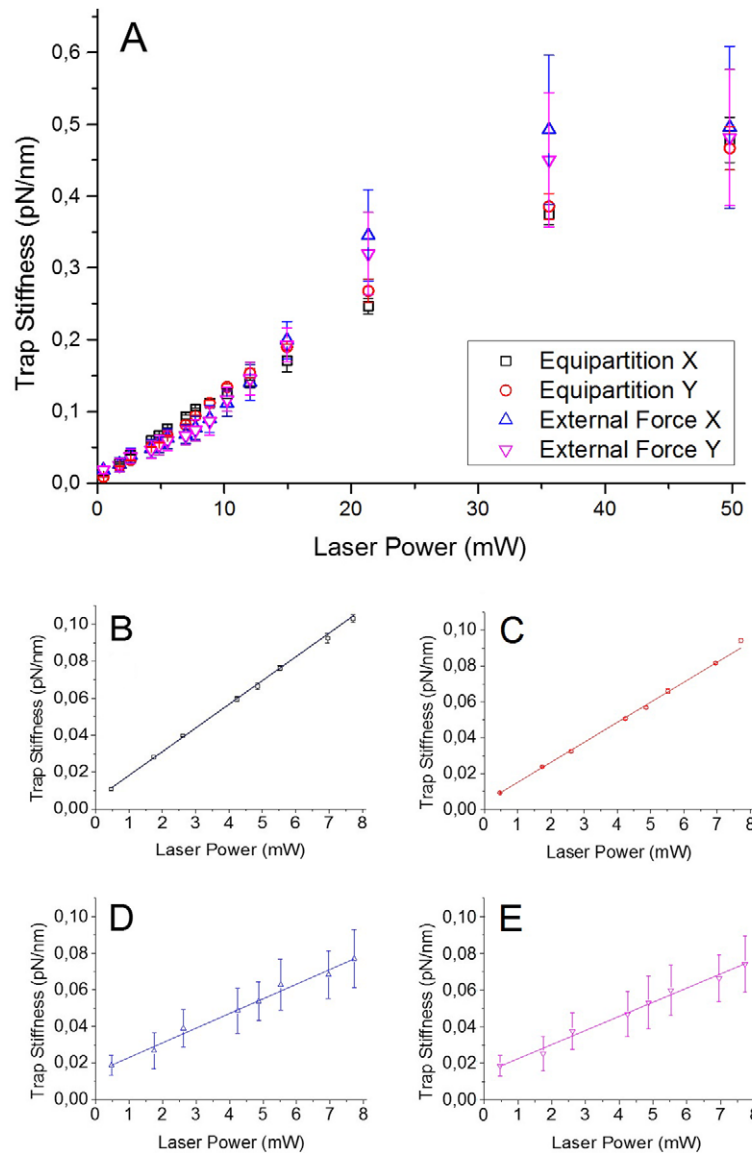
Figure 3. Dependence of trap stiffness on trapping laser power for a 1.0 μm polystyrene bead obtained by equipartition and external force calibration method in the range from 0.50 mW to 50.0 mW of laser power (A). Optical tweezers stiffness as a function of laser power (0.5–8.0 mW) and its best fit-line: equipartition along *X* axis (B), equipartition along *Y* axis (C), external force along *X* axis (D) and external force along *Y* axis (E). Every point in the graph is the average of 30 measurements.

The results obtained for laser power below 10 mW using the equipartition method confirm the previous calibration data highlighting the strong dependence between the laser power and the optical tweezers stiffness.

3.1.4. Calibration discussion. A comprehensive characterization of the QPD-based sensor has been provided and the high sensitivity and resolution of the detector has been confirmed by the experimental calibration. Nevertheless, it is possible to further increase the sensitivity and the resolution by improving the acquisition data system.

The optical tweezers stiffness usually depends on several experimental parameters such as the shape, refractive index and position of the trapped object, profile and intensity of the trapping laser and the sample medium refractive index. That is the reason why the optical tweezers stiffness was calculated by two different methods in the same experimental condition

and the relationship between trapping laser power and applied force was investigated. The basic calibration presented in this paper was the external force method. The results demonstrate that the minimum applicable and detectable force of the proposed optical tweezers is at least one order of magnitude better than the best result achieved by AFM. The external force method has allowed us to measure the highest applicable and detectable force by calculating the force necessary to escape the trapped particle from the optical tweezers focus spot. The escape force is proportional to the trapping laser beam power (table 1) and this confirms the possibility to analyse forces up to 11.17 pN using a 4.24 mW laser power and to use optical tweezers in a force range below the limit of detection of AFM. An alternative calibration method based on equipartition theory was carried out and the results obtained confirm the high sensitivity and resolution of the instrument (figure 3). The equipartition method is easy enough to implement, it is

very fast and does not require any additional equipment. After proper calibration it can be used to evaluate local temperature or/and to extend evaluation of Brownian motion into inertial ballistic regime [18].

We found that the calibration methods using external force and equipartition performed equally well in the reported experimental conditions. The reproducibility of calibration methods is expressed as the standard deviation of trap stiffness. The standard deviations obtained using external force are greater than the values calculated by the equipartition method for lower laser power (0.5 and 8.0 mW).

As it is possible to notice in figures 3(B) and (C), also the fitting straight lines calculated using the equipartition method have a non-zero intercept. The obtained fitted lines were not forced to pass through the origin point, even though they intersect the *Y* axis very close to the zero value, because this discrepancy from the theory highlights the small contribution from the detection laser during the particle trapping process to the final result. This effect is unavoidable in the proposed hybrid configuration because the presence of the AFM cantilever in the optical tweezers focal point area forces us to use a configuration based on a backscatter light detection system in which the 633 nm red laser beam is focused by the objective with minimal impact on the particle confinement. Furthermore, although the plots of trap stiffness as a function of beam power prove the linear relationship under 8 mW for the external force method results, the fit lines do not intersect the origin. This is not due to the presence of a trapping force in absence of the laser beam but to the inaccuracy of this method when it comes to extremely low laser power. In the external force approach zero stiffness is achieved if extremely small forces provoke the infinitely large Brownian movements. This is not reached, when we study the behaviour of a particle in flow, even in the absence of the trapping laser because there are frictional forces counter the free diffusion of the particle in the environmental liquid [32]. It evidences the advantage of the method based on of the trapped particles Brownian motion study when the trap weakness disturbs accuracy of the external force calibration technique. Indeed, when the laser is set on a lower power than 0.5 mW the force applied by the laser beam was frequently overcome by the drag force resulting from the slowest possible applied stage movement. Moreover, when the laser power is lower than 3 mW the fluctuations around the centre of the trap is comparable with the displacement of the particle due to the external drag force, affecting the precision of the result reached by the external force method (figures 3(D) and (E)). Our study pointed out that the trap stiffness values obtained using equipartition calibration have a directly proportional relationship with the trapping laser power and that the results are very precise and accurate in the region in which the force of the trap is weak. The curves obtained between 0.5 and 8.0 mW are well fitted by a line and the relative standard deviations rarely exceed 3% of the calculated trap stiffness. On the other hand this method appears to be less useful to measure the properties of the trap when trapping laser is set up at higher trapping power than 20 mW and this is quite evident considering that the stiffness-laser power correlation became non-linear at this point. The deviation of

the equipartition method curves from the drag force curves at high values of trapping laser power (figure 3(A)) is probably due to the sample heating [33], and possible deviations of the equipartition model from the diffusive regime into the ballistic interactions. We can therefore say that the use of few calibration techniques is crucial for measuring the optical tweezers stiffness in a wide range of applied trap power.

External force and equipartition calibration methods provide us only with information regarding the stiffness of the trap in the plane perpendicular to the incident lasers direction. Therefore a further 3D calibration has to be performed in order to fully understand the forces involved in particle confinement.

3.2. Applications examples

The developed hybrid atomic force microscope-optical tweezers allows us to manipulate micro and nanoscale systems and to analyse their material properties and behaviour from a different point of view. The proposed equipment is extremely versatile and it can be used in different configurations as required. The combination of atomic force microscopy and optical tweezers in one single piece of equipment enabled us to obtain images, manipulate and quantify motion and forces directly, during a single measurement.

In this paragraph we focus on two specific applications showing the methods used in these distinct experiments. In the first case, the trapping laser was used as a high precision nanomanipulator while the AFM cantilever guarantees the ability to visualize the treated sample zone with high resolution. The second experiment proved the possibility to detect force with femtonewton resolution, by using a colloidal cantilever as a manipulator and the optical tweezers system as a force and spatial sensor.

3.2.1. Nanomanipulation and high resolution imaging by AFM/ OT. One of the most interesting applications is to use tweezers in order to manipulate single objects (e.g. nanomaterials and cells). The main achievement of the optical trapping nanomanipulation was to develop a selective cell sorting process with the aim to purify samples and to study the biological behaviour of single selected cells. Nanomanipulation can also be useful to organize, assemble and locate complex hierarchical structures composed through optical tweezers manipulation. The proposed study is based on the capabilities of sorting single nano-objects using optical tweezers. In order to demonstrate the capabilities of the AFM/OT system we prepared a particle nanostructure using the dragging force of the trapping laser and we simultaneously scanned the sample using AFM.

First of all, the surface of the glass slide used in this experiment was functionalized with 3-aminopropyltriethoxysilane (APTES) using the method proposed by Labit *et al* [34]. The chemically functionalized glass coverslip was used in this experiment in order to increase the interface interaction between the 1.0 μm polystyrene bead and the substrate. During this experiment, the trapping laser power was set to 10 mW in order to reach a high trapping efficiency and avoiding convective flow or other undesirable phenomena which can affect
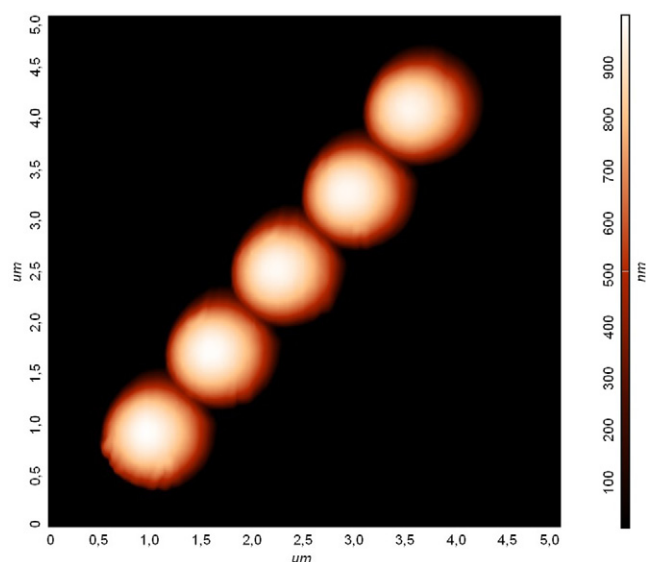
Figure 4. Topography image of polystyrene particles immobilized onto a special functionalized glass substrate obtained in tapping mode AFM using a HA_NC cantilever.

the nanomanipulation. First, five polystyrene particles were manoeuvred and isolated from the colloidal system, than the selected particles were individually confined in a clean water well and dragged to the glassy bottom of the channel in order to form a perfectly aligned straight line structure. The force exerted by the trapping laser is strong enough to push the particles to the glass wall and the adhesion effects allow to immobilize the particles to the substrate. The glass surface modification plays a crucial role in the proposed experiments. The attractive force between the positive charged surface and the negative charged polystyrene has an extremely beneficial influence on the stability of the produced structure. The AFM/OT system was used to collect AFM topographies of the area selected for conducting the experiment before and after the particle deposition as well as the surface of the single dragged particles.

Topography images of immobilizates were acquired in water using the tapping mode of AFM at a scan frequency of 0.2 Hz. Figure 4 shows a 5.0 μm × 5.0 μm AFM image of the ordered layer of polystyrene particles developed using the dragging force of the optical tweezer system.

This experiment allows to study the surface properties of the particles and substrates taking into consideration one single particle–surface interaction and studying single events to characterize locally the studied materials.

3.2.2. Combined atomic force microscopy and optical tweezers force sensor. Materials containing suspended microparticles or nanoparticles serve a wide variety of purposes and they are used in several applications. In all colloid system applications it is essential to maintain the colloid well dispersed and to avoid the formation of aggregates, therefore the knowledge, of the forces that regulate stability of particles in liquid, is fundamental. The equilibrium state and the hydrodynamic properties of colloid systems in an aqueous medium are affected by several environmental parameters (e.g. the

addition of salt influences the stability of colloids). An explanation for this fact was given by the Derjaguin–Landau–Verwey–Overbeek (DLVO) theory studying the surface charges at interfaces and the factors that affect the electrostatic double-layer force [35].

The possibility to detect extremely small forces (more than one order of magnitude lower than AFM) is certainly one of the most compelling strong points of the developed combined system.

In the following experiment, we demonstrate the possibility to use our hybrid instrument to quantify force in the femtonewton scale. As the research on the interaction forces acting between colloidal particles is very topical, the proposed configuration will be helpful to elucidate the details of the phenomena that regulate the colloids stability as well as the properties of molecules attached to their surface. Furthermore, the high number of scientific publications in this field gives us the possibility to highlight the advantages provided by the developed instrument in comparison to the most recent results obtained by using AFM only [36, 37].

Our colloidal probe cantilever was built following the 'Cantilever-moving technique' developed by Gan [38] in which a single fluorescent 5.5 μm particle was glued to the end of a tip-less AFM cantilever using a small amount of epoxy glue and the AFM head as a micromanipulator (figure 5(A)).

The experiments were performed inside a tailored PDMS microfluidic chip filled with water solutions at temperature 295 K. The single fluorescent colloid sphere fixed at the end of the tipless cantilever and a 1.0 μm fluorescent polystyrene sphere confined in the optical trap using 6.5 mW laser power, (figures 5(B)–(D)).

Before being used, all the materials were accurately cleaned rinsing carefully with acetone, isopropanol and water in order to remove any contaminate traces. The experiments were carried out by approaching the trapped particle with the AFM particle probe at a constant velocity (200 nm s^{-1}) in pure water and recording the optical tweezers output signals with a resolution of ±100 fN. The same experiment was repeated in 10^{-5} M and 10^{-3} M KCl solutions in that order. The particle approaches were performed after 30 min from the liquid introduction into the channel to reach the thermal equilibrium that was monitored by using a thermocouple inserted into the microchip channel. More than 30 approaches were performed per each analysed environmental condition in order to have statistically significant results. The acidity of the solutions was adjusted with small amounts of diluted KOH in order to reach pH 7.

The size and shape of the polystyrene particle mounted on the tipless cantilever have been accurately evaluated analysing top- and lateral-view micrographs collected by SEM prior to performing the experiment. Moreover, in order to correctly estimate the particle–particle distance, the analyzed trapped polystyrene sphere has been morphologically characterized immediately after the described experiment by AFM. The trapped particle surface has been studied applying the method described in the previous section.

The particles position and separation between the particles surfaces have been evaluated analysing both the white light
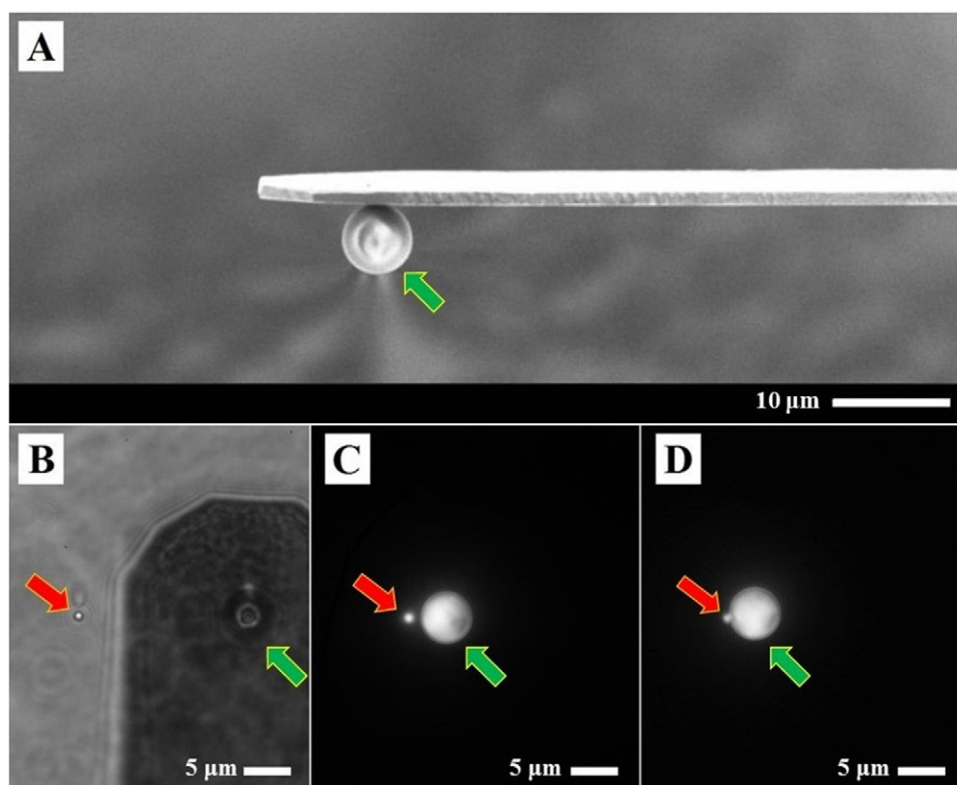
Figure 5. Overview of the applied setup and procedure for the single particles interaction study. A SEM micrograph of the 5.5 polystyrene particle mounted on the tipless AFM cantilever using AFM as a manipulator (A). A 1.0 μm polystyrene particle was trapped a few micrometers from the cantilever (B), then the probe was translated in the trapped particle direction (C) and finally the particle glued to the cantilever approached the surface of the trapped particle (D). Picture B was collected using a white light while pictures C and D were recorded using fluorescent particles excited by the green 532 nm wavelength laser. The red arrows indicate the position of the optically trapped 1 μm particle and the green arrows denote the location of the 5.5 μm particle attached to the AFM probe.

and fluorescence images, captured by the CMOS camera, using a custom-made LabVIEW algorithm capable of finding the center of the particles.

The force vs relative distance was obtained during the post-experiment data analysis, calculating the particle–particle distance with both optical microscope images and quadrant photodiode signals.

Measured force–distance relationship for different aqueous solutions at constant pH (figure 6) demonstrates the ability of our instrument to measure force, in the range typical for colloidal system with a subpiconewton resolution. The used configuration can quantify the forces of interaction between single particles with good reproducibility.

The developed combined atomic force microscopy and optical tweezers do not only have higher resolution and reproducibility than AFM during the analysis of the particles interaction forces [36] but the hybrid instrument also gives considerable advantages in relation to the experiment utility. Usually in the AFM investigations, the colloidal cantilever is used as external probe and force sensor to perturb and to study a layer of spheres deposited onto a solid surface [37]. The analysed particle is physically confined by other particles located in the analysed layer and by the surface in which it is placed producing a significant variation of the double layer compared to the theoretical situation where the single particle is dispersed in the surrounding liquid. On the other hand,

the experiment performed using the AFM/OT system allows miming the natural colloidal system condition in which the studied single particle is completely bordered by the liquid through the use of the optical trap, giving us a more reliable result.

Moreover, the obtained data (figure 6) confirm that the behaviour of colloidal systems observed experimentally agrees with the theoretical predictions. The DLVO theory assumed that the interaction between two particles is due to the sum of the electrostatic double-layer repulsion and the van der Waals attraction. At low salt concentration the double-layer repulsions are stronger than in pure water and the single polystyrene particles are stable. The particle stability increases with the KCl concentration in the micromolar scale.

The AFM/OT instrument was optimized to study extremely low forces, by increasing the sensitivity and limiting the detectable forces up to a maximum of a few pN. This configuration does not allow the detection of the, already well-known, interaction forces acting at very short particle–particle distances, but opens the way to study the long range interaction forces that are undetectable by using AFM only [36, 37]. As it is shown in figure 6, the attractive forces have a dominant effect for the particle–particle interaction experiments in pure water at pH = 7. In pure water, long range attraction is clearly measured, instead small short range repulsions that are still not strong enough to overcome the attractive component in the
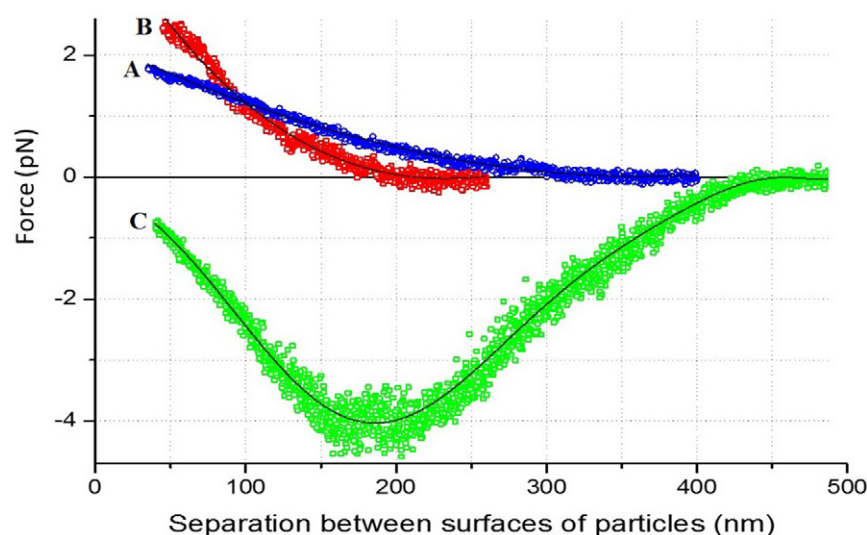
Figure 6. Force as a function of the relative distance between a single pair of polystyrene particles. The interaction force curves measured on approach between the polystyrene sphere attached to the AFM probe and the trapped sphere were collected varying KCl concentration: 10^{-3} M (blue circles; A), 10^{-5} M (red squares; B) and pure water (green triangles; C) at pH 7. The continuous lines correspond to the best fit in the particle–particle interaction range. The experiment was repeated more than 30 times in order to demonstrate the reproducibility of the technique.

analysed range. A completely different behaviour is observed in presence of KCl, where no final attractive forces act in the analysed range, while repulsive forces that grow exponentially with decreasing particle–particle distance are visible. In our experimental results, in all the studied systems, no interaction forces between the polystyrene particles could be observed at distances exceeding 450 nm.

The obtained experimental results confirm that the polystyrene particles colloid systems are more stable in a 10^{-3} M KCl solution, than a 10^{-5} M KCl solution and that is, in turn, more stable than the same system in water.

4. Conclusions and outlook

Atomic force microscopy is a versatile technique capable of covering a broad range of applications, but it is not able to detect small forces on the femtonewton scale due to technical limitations and restrictions. Based on this consideration, we have designed and developed a combined type of AFM-optical tweezers apparatus in order to build a high resolution imaging instrument capable to confine micro- and nanomaterial and to quantify force in the femtonewton scale. The successful development of the equipment has been described in detail and the calibration of the instrument has been presented in this study.

The setup presented in this article opens up the possibility to construct a combined atomic force microscope-optical tweezers which allows to manipulate biological systems of greater complexity and to analyse their material properties and behaviour from a different point of view, for example trapping and manipulating intracellular objects and probing the cell surface by AFM cantilever, simultaneously. This instrument will be useful for studying the mechanical properties of single long chain molecules, fibres and rods as it allows to analyse the effect of the twisting. By attaching a molecule (or a 1D nanomaterial) to the AFM cantilever on one side and to

a paramagnetic bead on the other it is possible to twist it using a rotating magnetic field to torque the bead. In this experiment the optical tweezers will act as a manipulator and the atomic force microscope as a force and spatial sensor.

The combination of atomic force microscopy and optical tweezers in one single piece of equipment has already given us the ability to obtain images, to manipulate and quantify the motion and the forces directly in the same sample. In the present study a few capabilities of the instrument has already been proved performing two detailed experiments, but it is expected that several applications will be found soon for the developed instrument thanks to his versatility and possibility to tackle challenge studies in extremely fascinating and crucial scientific topics including biophysics and nanosciences.

References

[1] Janshoff A, Neitzert M, Oberdorfer Y and Fuchs H 2000 Force spectroscopy of molecular systems—single molecule spectroscopy of polymers and biomolecules *Angew. Chem. Int. Ed. Engl.* **39** 3213–8 (PMID: 11028062)
[2] Voulgarakis N K, Redondo A, Bishop A R and Rasmussen K Ø 2006 Sequencing DNA by dynamic force spectroscopy: limitations and prospects *Nano Lett.* **6** 1483–7
[3] Neuman K C and Nagy A 2008 Single-molecule force spectroscopy: optical tweezers, magnetic tweezers and atomic force microscopy *Nat. Methods* **5** 491–6

[4] Ashkin A 1970 Acceleration and trapping of particles by radiation pressure *Phys. Rev. Lett.* **24** 156

[5] Ashkin A, Dziedzic J M, Bjorkholm J E and Chu S 1986 Observation of a single-beam gradient force optical trap for dielectric particles *Opt. Lett.* **11** 288–5

[6] Grier D G 1997 Optical tweezers in colloid and interface science *Curr. Opin. Colloid Interface Sci.* **2** 264–3

[7] Meiners J-C and Quake S R 2000 Femtonewton force spectroscopy of single extended DNA molecules *Phys. Rev. Lett.* **84** 5014

[8] Berthelot J, Acimovic S S, Juan M L, Kreuzer M P, Renger J and Quidant R 2014 Three-dimensional manipulation with scanning near-field optical nanotweezers *Nat. Nanotechnol.* **9** 295–9

[9] Visscher K, Schnitzer M J and Block S M 1999 Single kinesin molecules studied with a molecular force clamp *Nature* **400** 184

[10] Comstock M J, Ha T and Chemla Y R 2011 Ultrahigh-resolution optical trap with single-fluorophore sensitivity *Nat. Methods* **8** 335–40

[11] Lipfert J *et al* 2014 Double-stranded RNA under force and torque: Similarities to and striking differences from double-stranded DNA *Proc. Natl Acad. Sci. USA* **111** 15408–13

[12] Bennink M L, Leuba S H, Leno G H, Zlatanova J, de Grooth B G and Greve J 2001 Unfolding individual nucleosomes by stretching single chromatin fibers with optical tweezers *Nat. Struct. Biol.* **8** 606–7

[13] Shivashankara G V and Libchaber A 1997 Single DNA molecule grafting and manipulation using a combined atomic force microscope and an optical tweezer *Appl. Phys. Lett.* **71** 3727

[14] Huisstede J H, Subramaniam Vand Bennink M L 2007 Combining optical tweezers and scanning probe microscopy to study DNA–protein interactions *Microsc. Res. Tech.* **70** 26–33

[15] Jeffries G D M, Edgar J S, Zhao J, Shelby J P, Fong C and Chiu D T 2007 Using polarization shaped optical vortex traps for single-cell nanosurgery *Nano Lett.* **7** 415–2

[16] Wang X, Chen S, Kong M, Wang Z, Costa K D, Li R A and Sun D 2011 Enhanced cell sorting and manipulation with combined optical tweezer and microfluidic chip technologies *Lab Chip* **11** 3656

[17] Pang Y, Song H, Kim J H, Hou X and Cheng W 2014 Optical trapping of individual human immunodeficiency viruses in culture fluid reveals heterogeneity with single-molecule resolution *Nat. Nanotechnol.* **9** 624–30

[18] Huang R, Chavez I, Taute K M, Lukić B, Jeney S, Raizen M G and Florin E-L 2011 Direct observation of the full transition from ballistic to diffusive Brownian motion in a liquid *Nat. Phys.* **7** 576–80

[19] Yogesha, Bhattacharya S and Ananthamurthy S 2012 Characterizing the rotation of non symmetric objects in an optical tweezer *Opt. Commun.* **285** 2530–5

[20] Schäffer E, Nørrelykke S F and Howard J 2007 Surface forces and drag coefficients of microspheres near a plane surface measured with optical tweezers *Langmuir* **23** 3654–65

[21] Yao A, Tassieri M, Padgett M and Cooper J 2009 Microrheology with optical tweezers *Lab Chip* **9** 2568–75

[22] Nève N, Lingwood J K, Zimmerman J, Kohles S S and Tretheway D C 2008 The μPIVOT: an integrated particle image velocimeter and optical tweezers instrument for microenvironment investigations *Meas. Sci. Technol.* **19** 095403

[23] Cardinaels R and Stone H A 2015 Lubrication analysis of interacting rigid cylindrical particles in confined shear flow *Phys. Fluids* **27** 072001–22

[24] Xu S, Lou L, Li Y and Sun Z 2005 On the aggregation kinetics of two particles trapped in an optical tweezers *Colloids Surf.* A **255** 159–63

[25] Probst C, Grünberger A, Wiechert W and Kohlheyer D 2013 Microfluidic growth chambers with optical tweezers for full spatial single-cell control and analysis of evolving microbes *J. Microbiol. Methods* **95** 470–6

[26] Schneckenburger H, Hendinger A, Sailer R, Gschwend M H, Strauss W S, Bauer M and Schütze K 2000 Cell viability in optical tweezers: high power red laser diode versus Nd:YAG laser *J. Biomed. Opt.* **5** 40–4

[27] Abbondanzieri E A, Shaevitz J W and Block S M 2005 Picocalorimetry of transcription by RNA polymerase *Biophys. J.* **89** L61–3

[28] Mahamdeh M and Schäffer E 2009 Optical tweezers with millikelvin precision of temperature-controlled objectives and base-pair resolution *Opt. Express* **17** 17190–9

[29] Mills J P, Qie L, Dao M, Lim C T and Suresh S 2004 Nonlinear elastic and viscoelastic deformation of the human red blood cell with optical tweezers *Mech. Chem. Biosyst.* **1** 169–80 (PMID: 16783930)

[30] Rohrbach A 2005 Stiffness of optical traps: quantitative agreement between experiment and electromagnetic theory *Phys. Rev. Lett.* **95** 168102

[31] Tolić-Nørrelykke S F, Schäffer E, Howard J, Pavone F S, Jülicher F and Flyvbjerg H 2006 Calibration of optical tweezers with positional detection in the back focal plane *Rev. Sci. Instrum.* **77** 103101

[32] Sarshar M, Wong W T and Anvari B 2014 Comparative study of methods to calibrate the stiffness of a single-beam gradient-force optical tweezers over various laser trapping powers *J. Biomed. Opt.* **19** 115001–13

[33] Mao H, Ricardo Arias Gonzalez J R, Smith S B, Tinoco I Jr and Bustamante C 2005 Temperature control methods in a laser tweezers system *Biophys. J.* **89** 1208–316

[34] Labit H, Goldar A, Guilbaud G, Douarche C, Hyrien O and Marheineke K 2008 A simple and optimized method of producing silanized surfaces for FISH and replication mapping on combed DNA fibers *Biotechniques* **45** 469–58

[35] Maroto J A and de las Nieves F J 1998 Theoretical and experimental comparison of the colloid stability of two polystyrene latexes with different sign and value of the surface charge *Colloid. Polym. Sci.* **276** 453–8

[36] Lüderitz L A C and Klitzing R V 2013 Interaction forces between silica surfaces in cationic surfactant solutions: an atomic force microscopy study *J. Colloid. Interface Sci.* **402** 19–26

[37] Singh G, Bremmell K E, Griesserd H J and Peter K 2015 Colloid-probe AFM studies of the interaction forces of proteins adsorbed on colloidal crystals *Soft Matter* **11** 3188

[38] Gan Y 2007 Invited review article: a review of techniques for attaching micro- and nanoparticles to a probe's tip for surface force and near-field optical measurements *Rev. Sci. Instrum.* **78** 081101–8